J. Fluid Mech. (1986), *vol.* 162, *pp.* 53–67
Printed in Great Britain

Radiation of solitons by slender bodies advancing in a shallow channel

By C. C. MEI
Department of Civil Engineering, Massachusetts Institute of Technology, Cambridge, MA 02139, USA

(Received 7 January 1985)

It is known from recent experiments that the disturbance due to a slender ship advancing in a shallow channel is essentially one-dimensional in the horizontal plane. In particular solitons can be radiated upstream in a transient manner. In this note we develop a theory for soliton radiation by slender bodies. It is shown that, when the ship speed is in the transcritical range, one-dimensional upstream influence can occur even when the channel width is nearly of the order of the ship length but much greater than the ship beam. The theory is also extended to one or more ships travelling in the same channel at near-critical speeds.

1. Introduction

According to the classical linearized theory, a slender ship advancing steadily in an unbounded sea generates steady waves in its wake. In deep water there are two systems of waves: transverse and divergent; both are prominent only in a wedge-like wake of 19.28° half-angle. In finite depth h, when the Froude number $F = U/(gh)^{\frac{1}{2}}$ increases towards 1, the half-angle rises sharply towards 90°. If F increases beyond 1, the transverse waves disappear and the half angle slowly decreases from 90° (see Kostyukov 1958, figure 17, or Wehausen & Laitone 1960). The near critical speed ($F = 1$) the steady wave crests are nearly straight and perpendicular to the ship's axis.

It has long been observed experimentally that, in a channel of finite width and depth, a steadily advancing ship can radiate waves which propagate faster than the ship (Thews & Landweber 1935, 1936; Graff 1962† and Schmidt-Stiebitz 1966†). Interest in this type of upstream influence was rekindled recently by the systematic experiments of Huang *et al.* (1982). Much theoretical understanding has been gained by the two-dimensional (horizontal and vertical) studies of Wu & Wu (1982). By solving the transient Boussinesq equations numerically, they have demonstrated that an infinitely long surface-pressure band, advancing normally to its longitudinal axis, radiates solitons. This phenomenon is most pronounced when the speed of advance is fairly close to the critical speed. Akylas (1984) has shown, also for the same two-dimensional problem but for near-critical speeds, that the governing equations can be further simplified to an inhomogeneous KdV equation which can be more readily integrated numerically.

Ertekin (1984) and Ertekin, Webster & Wehausen (1984) have reported extensive three-dimensional experiments with a slender ship and pointed out the important correlation between soliton radiation and the 'blockage coefficient', which is the ratio

† These references were pointed out to the author by Professor J. V. Wehausen.

of the maximum cross-sectional area of the ship to the cross-sectional area of the channel. They have also performed computations similar to those of Wu & Wu for the pressure band and for a two-dimensional body towed along the bottom. Why a slender ship can generate long-crested solitons in a wide channel remains to be studied, however. Numerical solutions to transient two-dimensional equations due to Green & Nagdi, which resemble those of Boussinesq, are being carried out by Ertekin (1985, private communication) for a moving pressure patch of rectangular plan form. Since it is not a simple matter to establish the quantitative correspondence between a pressure patch and a ship, there is a need for a more analytical theory connecting directly the three-dimensional geometry of the ship and the channel to the one-dimensional solitons.

The observation by Ertekin *et al.* that the tendency of soliton radiation is related to the blockage coefficient implies that the finite channel width is an important parameter of the problem. Some time ago Mei (1976) developed a nonlinear dispersive three-dimensional theory for a slender ship in shallow water. However, he treated only a laterally unbounded sea and the steady state. In view of the experiments mentioned above we need to modify it to include time dependence and the effect of finite channel width; this is carried out first for a vertical strut of half-beam B and half-length L, in §2. Two dimensionless parameters are found to be important: $\alpha = (1-F^2)/2\mu^2$ and $\beta = B/W\mu^4$, where $\mu = h/L$ and $W =$ half channel width. When α and β are of order unity, the motion is found to be horizontally one-dimensional, to leading order, both ahead and behind the strut. Furthermore, the free surface satisfies an inhomogeneous KdV equation in which the forcing term is related to the blockage coefficient B/W through β. Numerical results are then discussed and compared with the experiments of Ertekin *et al.* for much greater β. Reasonable agreement is nevertheless found for the upstream phenomenon. The theory is further extended to several ships and sample results for two ships in tandem are presented.

2. Asymptotic equation for one ship in a wide channel

Let the ship advance at the constant speed U, immediately after $t^* = 0$, along the centreline of a channel of depth h and half-width W. Only one half of the channel $0 < y^* < W$ will be considered.

In the reference frame fixed on the ship the velocity potential $\phi^*(x^*, y^*, z^*, t^*)$ is governed by the following equations:

$$\left(\frac{\partial^2}{\partial x^{*2}}+\frac{\partial^2}{\partial y^{*2}}+\frac{\partial^2}{\partial z^{*2}}\right)\phi^* = 0 \quad (-h^* < z^* < \zeta^*) \tag{2.1}$$

in the fluid;

$$\frac{\partial \phi^*}{\partial t^*}+g\zeta^*+U\frac{\partial \phi^*}{\partial x^*}+\tfrac{1}{2}(\nabla^*\phi^*)^2 = 0 \quad (z^* = \zeta^*), \tag{2.2}$$

$$\frac{\partial \zeta^*}{\partial t^*}+U\frac{\partial \zeta^*}{\partial x^*}+\frac{\partial \phi^*}{\partial x^*}\frac{\partial \zeta^*}{\partial x^*}+\frac{\partial \phi^*}{\partial y^*}\frac{\partial \zeta^*}{\partial y^*} = \frac{\partial \phi^*}{\partial z^*} \quad (z^* = \zeta^*) \tag{2.3}$$

on the free surface; and

$$\frac{\partial \phi^*}{\partial z^*} = 0 \quad (z^* = -h^*) \tag{2.4}$$

on the sea bottom. To demonstrate the essential features in the far field of a slender ship, it is enough to consider a wall-sided ship, i.e. a *strut* with vertical walls extending the entire sea depth. As will be remarked in §2, it is always possible to adjust the beam of an equivalent strut so that it has the same blockage coefficient as a slender ship with draught less than the water depth. The boundary condition on the strut is then

$$\left.\begin{aligned}\frac{\partial\phi^*}{\partial y^*} &= \left(U+\frac{\partial\phi^*}{\partial x^*}\right)\frac{\partial Y^*}{\partial x^*} \quad \text{on } y^* = Y^*(x^*) \quad (-L < x^* < L),\\ &= 0 \qquad\qquad\qquad\qquad \text{on } y^* = 0 \quad (|x^*| > L).\end{aligned}\right\} \tag{2.5}$$

Along the channel wall the normal flux must vanish:

$$\frac{\partial\phi^*}{\partial y^*} = 0 \quad (y^* = W, \quad \text{all}\, x^*). \tag{2.6}$$

For ahead of and behind the ship we must have

$$\zeta^*, \nabla^*\phi^* \to 0 \quad (x^* \to \pm\infty, t < \infty). \tag{2.7}$$

The initial condition is

$$\zeta^*, \nabla^*\phi^* = 0 \quad (t^* = 0) \tag{2.8}$$

everywhere in the fluid.

We shall normalize all the variables as follows:

$$\left.\begin{aligned}\zeta^* = A\zeta, \quad \phi^* = \left(\frac{gAL}{U}\right)\phi, \quad x^* = Lx, \quad y^* = Ly,\\ z^* = hz, \quad t^* = \frac{L}{(gh)^{\frac{1}{2}}}t, \quad Y^* = BY,\end{aligned}\right\} \tag{2.9}$$

where A is the typical wave amplitude, yet undefined, L is the half-length, and B the half-beam, of the strut.

Let us denote

$$\mu = \frac{h}{L}, \quad \epsilon = \frac{A}{h}, \tag{2.10}$$

both of which are assumed to be small. The dimensionless form of (2.1)–(2.5) can now be written

$$\mu^2\Delta\phi + \phi_{zz} = 0 \quad (-1 < z < \epsilon\zeta), \tag{2.11}$$

where

$$\Delta \equiv \frac{\partial^2}{\partial x^2} + \frac{\partial^2}{\partial y^2},$$

$$F^2\mu^2\zeta + F\mu^2(\phi_t + F\phi_x) + \frac{1}{2}\epsilon\,[\mu^2(\phi_x^2+\phi_y^2)+\phi_z^2] = 0 \quad (z = \epsilon\zeta), \tag{2.12}$$

$$\phi_z = \mu^2 F(\zeta_t + F\zeta_x) + \epsilon(\phi_x\,\zeta_x + \phi_y\,\zeta_y) \quad (z = \epsilon\zeta), \tag{2.13}$$

$$\phi_z = 0, \quad (z = -1), \tag{2.14}$$

and

$$\phi_y = \frac{1}{\epsilon}\frac{B}{L}[F^2 + \epsilon\phi_x]\,Y_x \quad \text{on } y = \frac{B}{L}\,Y. \tag{2.15}$$

As usual, the following Taylor expansion is introduced

$$\phi = \phi_0 - \tfrac{1}{2}\mu^2(z+1)^2\,\Delta\phi_0 + \frac{\mu^4}{4!}(z+1)^4\,\Delta\Delta\phi_0 + \ldots, \tag{2.16}$$

which satisfies (2.11) and (2.14). Keeping terms of order $O(\epsilon)$ and $O(\mu^2)$ we get from (2.12) and (2.13):

$$\mathrm{D}\phi_0 + F\zeta = \frac{\mu^2}{2!}\,\Delta(\mathrm{D}\phi_0) - \frac{\epsilon}{2F}(\phi_{0x}^2 + \phi_{0y}^2) \tag{2.17}$$

$$F\,\mathrm{D}\zeta + \Delta\phi_0 = -\epsilon\zeta\,\Delta\phi_0 + \tfrac{1}{6}\mu^2\Delta\Delta\phi_0 - \epsilon(\phi_{0x}^2\,\zeta_x + \phi_{0x}\,\zeta_y) \tag{2.18}$$

where D is the operator $$\mathrm{D} = \frac{\partial}{\partial t} + F\frac{\partial}{\partial x}.$$

If ζ is eliminated from (2.17) and (2.18) we obtain

$$\Delta\phi_0 - \mathrm{D}^2\phi_0 - \frac{\epsilon}{2F}\mathrm{D}(\phi_{0x}^2 + \phi_{0y}^2) - \frac{\epsilon}{F}\nabla\cdot[(\mathrm{D}\phi)\,\nabla\phi] + \mu^2(\tfrac{1}{2}\Delta\mathrm{D}^2\phi_0 - \tfrac{1}{6}\Delta\Delta\phi_0) = O(\epsilon^2, \epsilon\mu^2, \mu^4). \quad (2.19)$$

Defining the depth-averaged $\bar{\phi}$ by

$$\bar{\phi} = \frac{1}{(1+\epsilon\zeta)}\int_{-1}^{\epsilon\zeta} \phi\,\mathrm{d}z \quad (2.20)$$

we find $$\phi_0 = \bar{\phi} + \tfrac{1}{6}\mu^2\,\Delta\bar{\phi} + O(\epsilon\mu^2, \mu^4), \quad (2.21)$$

which is used to rewrite (2.19):

$$\Delta\bar{\phi} - \mathrm{D}^2\bar{\phi} - \frac{\epsilon}{2F}\mathrm{D}(\bar{\phi}_x^2 + \bar{\phi}_y^2) - \frac{\epsilon}{F}\nabla\cdot[(\mathrm{D}\bar{\phi})\,\nabla\bar{\phi}] + \tfrac{1}{3}\mu^2\mathrm{D}^2\Delta\bar{\phi} = O(\epsilon^2, \epsilon\mu^2, \mu^4). \quad (2.22)$$

This is the asymptotic equation containing leading-order effects of dispersion and nonlinearity. If $\partial/\partial t = 0$, (2.22) reduces to Mei (1976, equation 7).

If we assume that B/L is at most of order $O(\epsilon)$, then to leading order the boundary condition (2.15) on the body is

$$\frac{\partial\bar{\phi}}{\partial y} = \frac{B}{\epsilon L}\,F^2\,Y_x \quad \text{on } y = 0. \quad (2.23)$$

For arbitrary F, one must solve numerically the two-dimensional equation (2.22), subject to the conditions (2.23), (2.6), (2.7) and (2.8). This is a complicated numerical task.

We shall focus attention on the neighbourhood of the critical speed, as in Mei (1976). Since to leading order (2.22) may be rewritten

$$(1-F^2)\,\bar{\phi}_{xx} + \bar{\phi}_{yy} - (\bar{\phi}_{tt} + 2F\bar{\phi}_{xt}) = O(\epsilon, \mu^2), \quad (2.24)$$

where the right-hand side represents nonlinearity and dispersion, we assume

$$1 - F^2 = 2\alpha\mu^2, \quad (2.25)$$

where $\alpha = O(1)$, in order that the linear term $\bar{\phi}_{xx}$ be comparable with the nonlinear and dispersive terms. Because soliton radiation must involve nonlinearity and dispersion at large time, the term $\bar{\phi}_{xt}$ which involves the lowest-order time derivative is more important than $\bar{\phi}_{tt}$ and can only be of order $O(\mu^2)$. Thus we let

$$\tau = \mu^2 t. \quad (2.26)$$

Without introducing additional restrictions we also set

$$\epsilon = \mu^2, \quad (2.27)$$

which defines the amplitude scale $$A = \frac{h^3}{L^2}. \quad (2.28)$$

We now renormalize y as follows:

$$y = \frac{\eta}{\mu^m\,\eta_0}, \quad (2.29)$$

with $\eta_0 = O(1)$, and
$$\frac{1}{\mu^m \eta_0} = \frac{W}{L}, \tag{2.30}$$
so that the channel wall is along the line $\eta = 1$. With (2.25)–(2.27) and (2.29), (2.22) becomes
$$\frac{\partial^2 \bar{\phi}}{\partial \eta^2} = -\frac{\mu^{2-2m}}{\eta_0^2}\left[2\alpha\bar{\phi}_{xx} - 2\bar{\phi}_{\tau x} - 3\bar{\phi}_x\bar{\phi}_{xx} + \tfrac{1}{3}\bar{\phi}_{xxxx}\right] + O(\mu^{4-4m}), \tag{2.31}$$
while (2.23) becomes
$$\frac{\partial \bar{\phi}}{\partial \eta} = \frac{1}{\epsilon\mu^m \eta_0}\frac{B}{L} Y_x = \frac{BW}{h^2} Y_x. \tag{2.32}$$

As long as $1-m > 0$ and $BW/h^2 < O(1)$, $\bar{\phi}$ is independent of η to leading order. We may choose for example $m = \frac{1}{2}$ so that
$$2(1-m) = 1, \quad y = \frac{\eta}{\mu^{\frac{1}{2}}\eta_0}, \tag{2.33}$$
and define an $O(1)$ coefficient b by
$$\frac{BW}{h^2} = b\mu. \tag{2.34}$$

Now let us expand $\bar{\phi}$ as a power series in μ:
$$\bar{\phi} = \Phi_0 + \mu\Phi_1 + \dots. \tag{2.35}$$
Clearly,
$$\Phi_0 = \Phi_0(x, \tau) \tag{2.36}$$
at order $O(1)$. At the order $O(\mu)$ Φ_1 satisfies
$$\frac{\partial^2 \Phi_1}{\partial \eta^2} = -\frac{1}{\eta_0^2}\{2\alpha u_x - 2u_\tau - 3uu_x + \tfrac{1}{3}u_{xxx}\}, \tag{2.37}$$
$$\frac{\partial \Phi_1}{\partial \eta} = bY_x \quad (\eta = 0), \tag{2.38}$$
$$\frac{\partial \Phi_1}{\partial \eta} = 0 \quad (\eta = 1), \tag{2.39}$$
where
$$u \equiv \Phi_{0x}. \tag{2.40}$$
Integrating (2.37) from $\eta = 0$ to 1 and using (2.38) and (2.39) we obtain an inhomogeneous KdV equation:
$$-u_\tau + \alpha u_x - \tfrac{3}{2}uu_x + \tfrac{1}{6}u_{xxx} = \tfrac{1}{2}b\eta_0^2 Y_x \quad (-\infty < x < \infty). \tag{2.41}$$
From (2.11), the leading-order free-surface height is
$$\zeta = -\Phi_{0x} + O(\mu). \tag{2.42}$$
Let
$$\beta = b\eta_0^2 = \frac{B}{W}\Big/\mu^4 = O(1). \tag{2.43}$$

We finally have an inhomogeneous KdV equation
$$\zeta_\tau - \alpha\zeta_x - \tfrac{3}{2}\zeta\zeta_x - \tfrac{1}{6}\zeta_{xxx} = \tfrac{1}{2}\beta Y_x \quad (-\infty < x < \infty), \tag{2.44}$$

which depends on two parameters: α representing the ratio of detuning to nonlinearity or dispersion (cf. (2.25)) and β representing the ratio of the blockage coefficient to nonlinearity or dispersion. In (2.41), the function on the right is in the normalized horizontal fluid flux due to the change of cross-sectional area of the strut. If the body is a ship with a draught smaller than water depth, we need only change Y_x to S_x, where S is the dimensionless cross-sectional area $S^*/S_{\max}$ of the ship, and reinterpret the blockage coefficient B/W as $S_{\max}/2Wh$. This assertion can be more formally established by a matched-asymptotics argument. Since we shall not be interested in the near field of the ship ($y^2+z^2 = O(S_{\max})$), these details will not be presented here.

The homogeneous KdV equation admits the following soliton solution:

$$\zeta = \zeta_0 \operatorname{sech}^2 \tfrac{1}{4}(3\zeta_0)^{\frac{1}{2}} (x+C\tau), \tag{2.45}$$

where the phase speed relative to the ship is

$$C = \tfrac{1}{2}\zeta_0 + \alpha. \tag{2.46}$$

Recall from (2.25) that $\alpha > 0$ (or < 0) for sub-(or super-)critical speed. Thus for the same soliton amplitude ζ_0, C increases as the ship reduces its speed. In particular C can be zero if $\alpha = -\frac{1}{2}\zeta_0$ or, equivalently,

$$F^2 = 1+\mu^2\zeta_0. \tag{2.47}$$

In his two-dimensional problem with a pressure band on the free surface, Akylas (1984) obtained an equation similar to (2.44); there Y_x is replaced by the first derivative of a δ-function; and β is replaced by the total force (i.e. the integral of the pressure). Since β here is proportional to the blockage coefficient B/W we see at once that the inhomogeneous term, and hence soliton generation, is appreciable only if B is not too small (or W not too large). But the condition $B/W = O(\mu^4)$ clearly allows the theory to be of practical interest. If all other parameters are the same, increasing ship length also strengthens the forcing.

Equation (2.44) is of course simple to integrate numerically and can exhibit the primary physical feature of soliton radiation.

3. Extensions for several ships in a canal

Let there be a ship i that is cruising at the speed $U+V_i$ to the left along the line $y^* = y_i^*$.

In the coordinate system moving at speed U the effective beam of ship i is described by

$$y^* = y_i^* \pm B_i\, Y^i(x^* + V_i t^*) \quad (x_{\mathrm{B}}^{i*} < x^* < x_{\mathrm{S}}^{i*}), \tag{3.1}$$

where x_{B}^{i*} and x_{S}^{i*} respectively denote the bow and stern of ship i. We assume that the relative speed V_i is no greater than $O(\mu(gh)^{\frac{1}{2}})$. The channel walls are along $y^* = -W$ and $y^* = W$. The assumptions (2.30) and (2.33) are kept, so that the channel width is much greater than the characteristic ship length.

In the normalized variables of (2.9), the exact boundary condition on ship i reads

$$\frac{\partial\bar{\phi}}{\partial y} = \pm\frac{B_i}{L}\frac{1}{\epsilon}\left[F^2\left(1+\frac{V_i}{U}\right)+\epsilon\phi_x\right] Y_x^i \quad \text{on } y = y_i \pm \frac{B_i}{L}\, Y^i(x), \tag{3.2}$$

which can be simplified under (2.34) and $V_i/U < O(\mu)$ to

$$\frac{\partial\bar{\phi}}{\partial\eta} = \pm\frac{B_i W}{h^2}\, Y_x^i + O(\mu^2) \quad \text{along } \eta = \eta_i \pm 0 \quad (x_{\mathrm{B}}^i < x < x_{\mathrm{S}}^i), \tag{3.3}$$

where $\max Y^i = 1$. It is worth noting that the slightly unequal ship speeds do not alter the quasi-steady form of the boundary condition on the ship, to leading order.

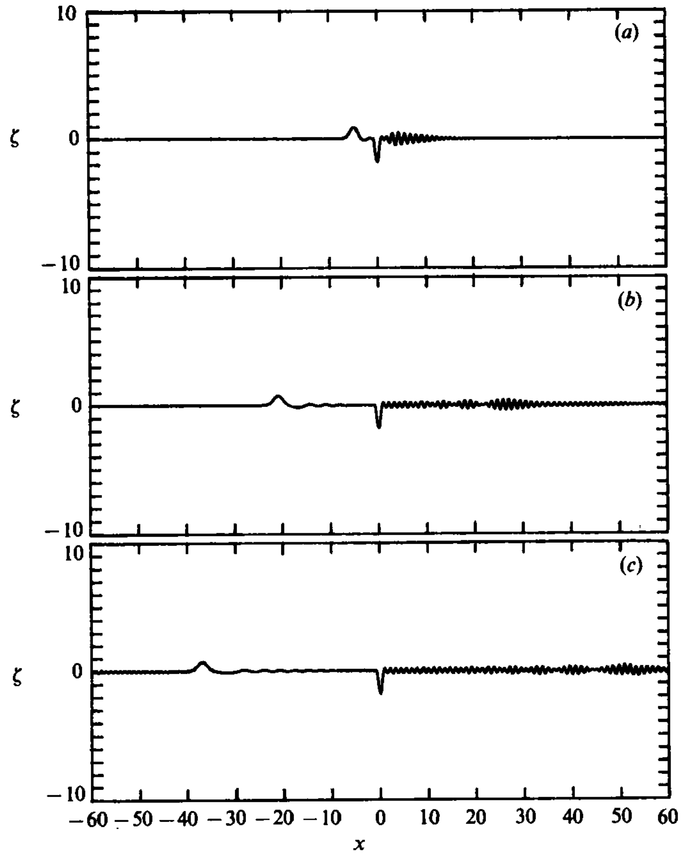

FIGURE 1. Evolution of free surface due to one strut. From bow to stern $-1 < x < 1$, $\beta = 10.4$, $\alpha = 5$ (low subcritical speed). (*a*) $\tau = 1$, (*b*) 3, (*c*) 5.

The same perturbation procedure then leads to the following inhomogeneous KdV equation:

$$\zeta_\tau - \alpha\zeta_x - \tfrac{3}{2}\zeta\zeta_x - \tfrac{1}{6}\zeta_{xxx} = \tfrac{1}{2}\sum_{i=1} \beta_i\, Y^i_x; \tag{3.4}$$

where

$$\beta_i = B_i / W\mu^4. \tag{3.5}$$

The forcing term is the sum of forcing terms of individual ships; the lateral positions (y_i or η_i) of their centrelines are unimportant.

4. Numerical results for one ship

The explicit finite-difference scheme of Johnson (1972) has been employed. In all computations we have taken $\Delta x = 0.1$ and $\Delta\tau = 0.0009$.

The measurements reported in Ertekin (1984) and Ertekin *et al.* (1984) were for a wide range of water depths and channel widths, ship draughts and ship speeds. The ship length was kept the same, $2L = 152.4$ cm. The ship hull is of the class Series 60, Block 80† and the blockage coefficient S_B is defined to be the ratio of the maximum

† Detailed geometry of this ship form has been standardized by, and is available from, the US Society of Naval Architecture and Marine Engineering (SNAME).

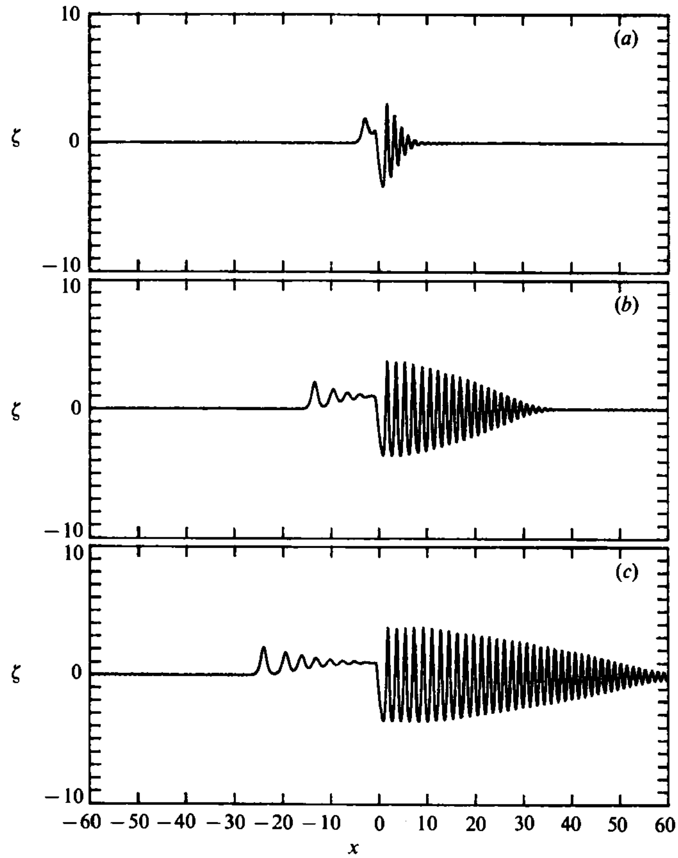

FIGURE 2. Evolution of free surface due to one strut, $\beta = 10.4$, $\alpha = 2.5$ (subcritical speed). (*a*) $\tau = 1$, (*b*) 2, (*c*) 3.

cross-sectional area of the ship to the area of the channel $2hW$. To allow comparison with theory we simply replace S_B by our B/W, and interpret the rate of beam variation as the rate of change of the cross-sectional area. The dimensions in all the experiments correspond to very large β, much beyond the intended realm of our theory.

Two cases with the smallest β are nevertheless chosen for comparison with our theory. The geometrical parameters are:

(i) $h = 15$ cm, $W = 244$ cm, $2L = 152.4$ cm, $S_B = 0.0157$, $\mu^2 = 0.03875$, $\beta = 10.4$;

(ii) $h = 12.5$ cm, $W = 244$ cm, $2L = 152.4$ cm, $S_B = 0.0188$, $\mu^2 = 0.02691$, $\beta = 26.0$.

In particular the theoretical strut has a half-beam which varies parabolically along x, i.e.

$$Y(x) = 1 - x^2. \tag{4.1}$$

Therefore the strut is equivalent to the model ship grossly but not in detail.

The evolution of the free surface for the case $\beta = 10.4$ is typical. For a very low subcritical speed $\alpha = 5$, figure 1 (*a–c*), only one small soliton is discernible upstream. Along the ship there is a local low water which becomes steady as time passes. In the wake there is a packet of waves oscillating about $z = 0$. The packet lengthens with time and the waves near the ship approach a steady uniform amplitude. For a high subcritical speed, $\alpha = 2.5$, figure 2 (*a–c*), more crests are radiated upstream. They

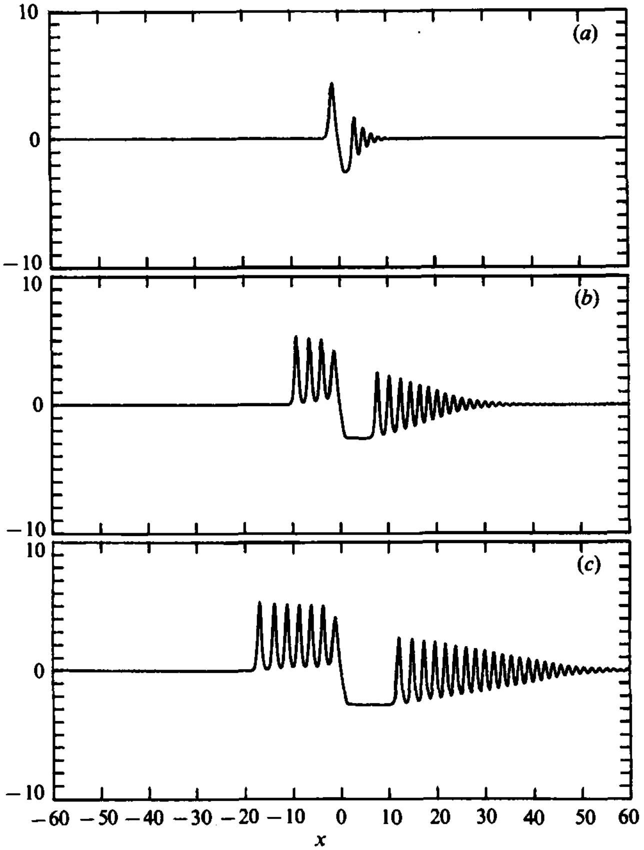

FIGURE 3. Evolution of free surface due to one strut, $\beta = 10.4$, $\alpha = 0$ (critical speed). (*a*) $\tau = 1$, (*b*) 3, (*c*) 5.

march ahead in order of decreasing height. The leading crest becomes a separate soliton first, while the trailing crests have a mean sea level slightly above $z = 0$, resembling an undular bore. After a still longer time, the second crest sheds its tail and becomes a separate soliton lower than the first. Downstream of the ship, the free surface oscillates at large amplitude about the mean sea level $z = 0$; the envelope also lengthens with time.

Figure 3(*a–c*) shows the evolution at the critical speed $\alpha = 0$. High-frequency solitons are quick to form at high frequency upstream, and eventually attain the same height. There is now a region of low water near and behind the ship followed by a packet of waves oscillating about $z = 0$. The low-water region and the wave packet extend with time.

For a low supercritical speed $\alpha = -2.5$, figure 4(*a–c*), the qualitative features resemble those of the critical case with a slower rate of radiation but a greater soliton amplitude.

All these features are in qualitative accordance with the records of Ertekin taken from gauges fixed along a wave tank.

For a sufficiently high supercritical speed such as $\alpha = -5.0$, no solitons are radiated, see figure 5(*a–c*). Near the ship a local steady-state rise is quickly established, which corresponds to the solution to (2.44) with $\zeta_\tau = 0$. A transient wave packet is shed in the wake with the usual signs of frequency dispersion.

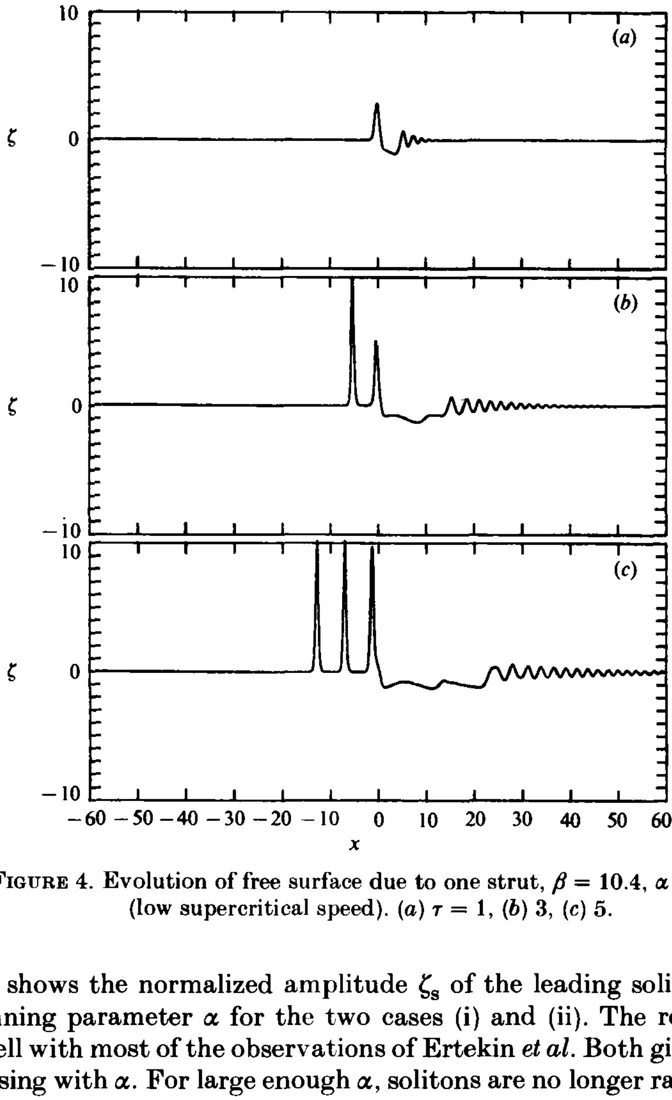

FIGURE 4. Evolution of free surface due to one strut, $\beta = 10.4$, $\alpha = -2.5$ (low supercritical speed). (a) $\tau = 1$, (b) 3, (c) 5.

Figure 6 shows the normalized amplitude ζ_s of the leading soliton as a function of the detuning parameter α for the two cases (i) and (ii). The results are seen to compare well with most of the observations of Ertekin *et al.* Both give the same trend of ζ_s increasing with α. For large enough α, solitons are no longer radiated, according to our theory; the cutoff values are marked in figure 6. In the experiments high solitons (sometimes with breaking) were still observed. This discrepancy occurs at values of α quite beyond the realm of our theory. Equation (2.22), which is less restrictive with respect to α, would probably yield better agreement for a wider range of α. Note also that this good agreement is for the wave field ahead of the ship only. Behind the ship Ertekin's recorded wave patterns were quite two-dimensional. This is probably the result of the relatively large blockage coefficient. A different theory based on the fuller equation (2.22) or its equivalent is needed in order to reproduce all the downstream features in Ertekin's experiments. For the parameter range defined by (2.25) and (2.43), our theory gives one-dimensional waves both ahead and behind the ship.

Since, for $\alpha \leqslant 0$ ($F \geqslant 1$), the radiated solitons ultimately approach the same amplitude advancing at the same speed, there appears to be an asymptotic steady state, in which the distance between two successive solitons can be defined as the wavelength of the soliton train. The existence of a constant 'wavelength' is consistent

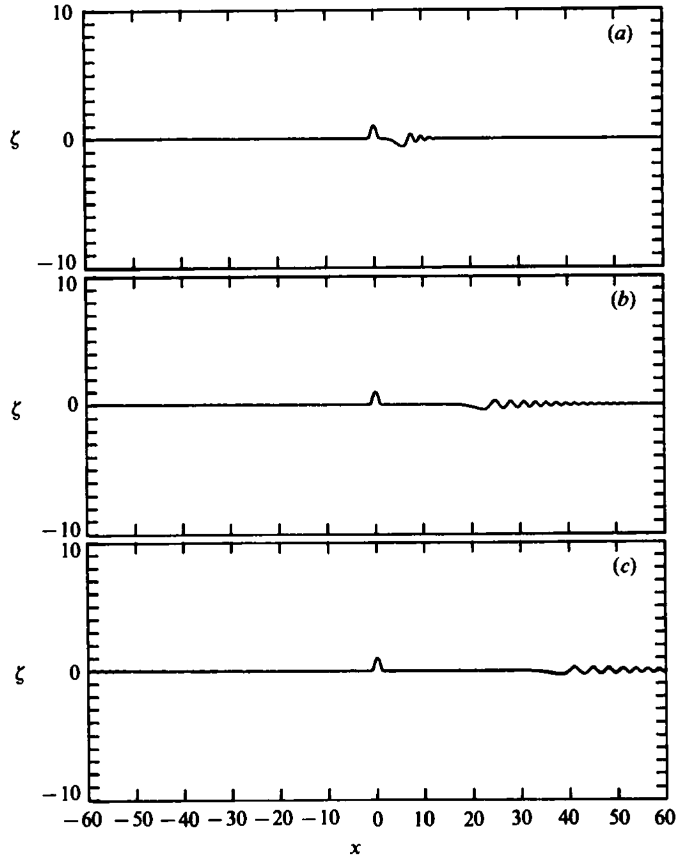

FIGURE 5. Evolution of free surface due to one strut, $\beta = 10.4$, $\alpha = -5$ (high supercritical speed). (*a*) $\tau = 1$, (*b*) 3, (*c*) 5.

with the known result that two non-overlapping solitons do not interact, within the approximation of the KdV equation. Dividing the asymptotic wavelength by the soliton phase speed which, in dimensionless form and stationary frame of reference, is

$$\frac{C}{(gh)^{\frac{1}{2}}} = F + \mu^2(\tfrac{1}{2}\zeta_0 + \alpha),$$

we can get the asymptotic wave period. For $\alpha > 0$ ($F < 1$) the upstream solitons are unequal in height; there cannot be a steady-state wavelength or period. Ertekin (1984) and Ertekin *et al.* (1984) have taken the difference in arrival times of the first two crests recorded at a fixed station as the measured period of soliton radiation T_f. For the two cases with which we have compared our theory, these gauges were so near (< 20 m) to the bow initially, owing to the limited length of tank, that the leading crests in the last record were still not separated (for case (i), see pp. 300–302, Ertekin 1984). Therefore, their period of radiation is not related to our steady-state period, even after proper transformation of coordinates. Nevertheless, both our calculations and their experiments show the qualitative trend of soliton period increasing with ship speed, for supercritical speeds.

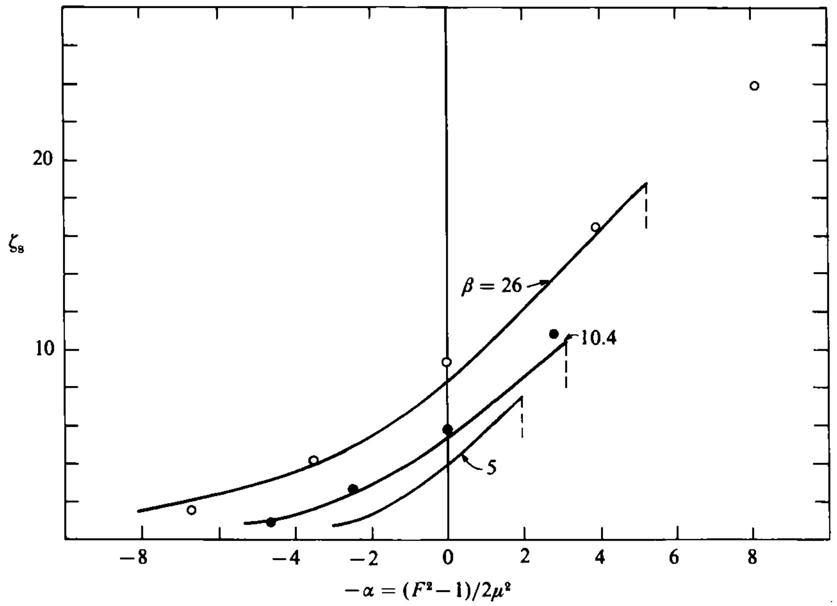

FIGURE 6. Amplitude of leading soliton *versus* α: ——, theory; ○, ●, experiments. Vertical dashes mark the cutoff of soliton radiation.

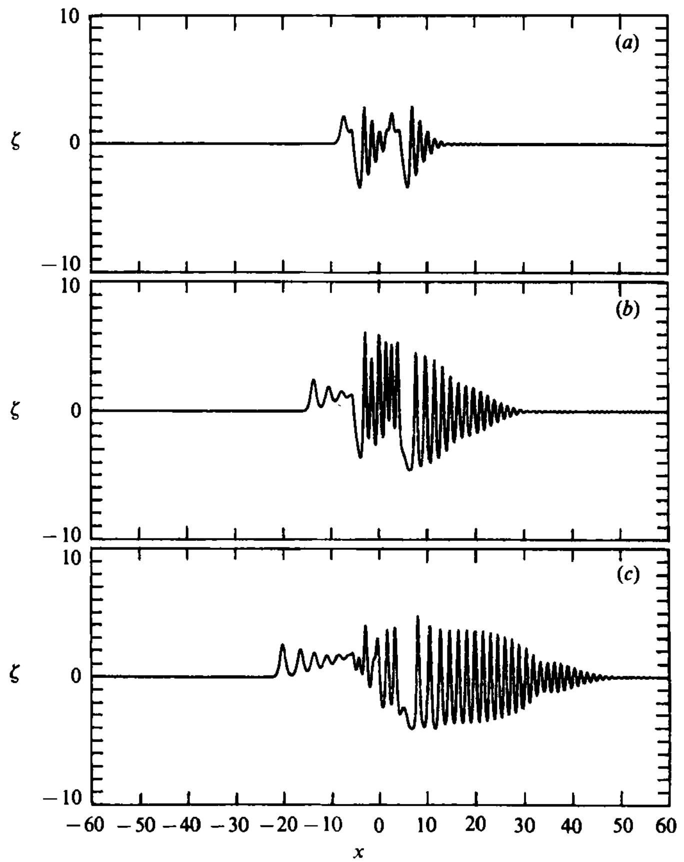

FIGURE 7. Evolution of free surface due to two identical ships in tandem. Ships are located in $-6 < x < -4$, $4 < x < 6$, $\beta = 10$, l/L = (centre-to-centre spacing)/L = 10, $\alpha = 2$. (*a*) $\tau = 1$, (*b*) 2, (*c*) 3.

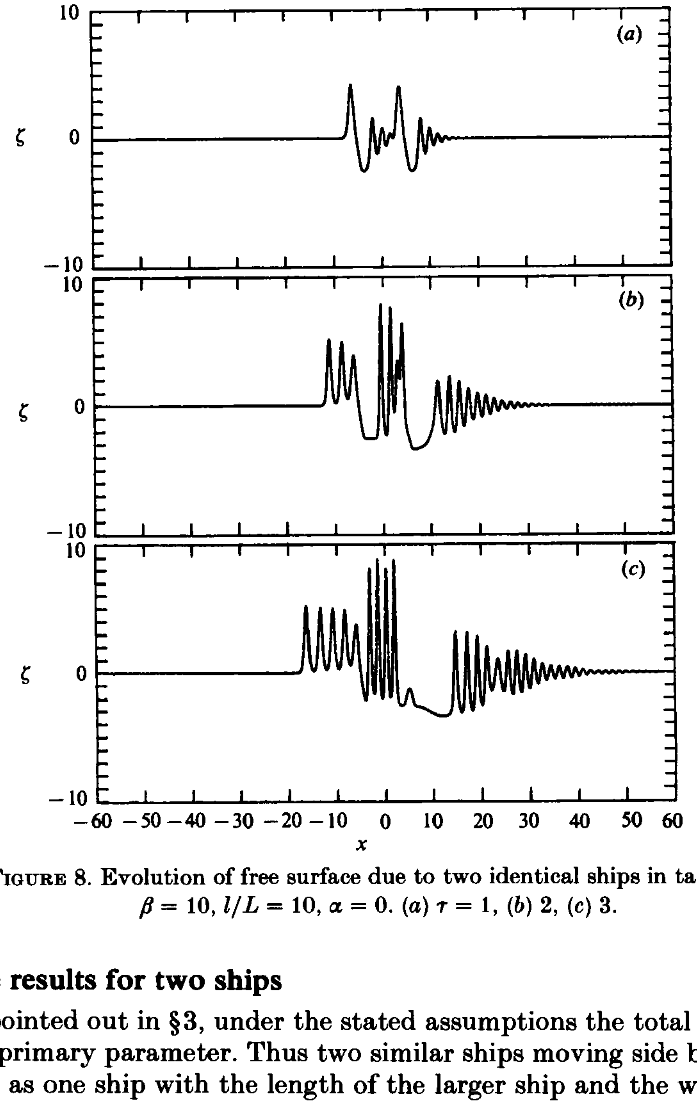

FIGURE 8. Evolution of free surface due to two identical ships in tandem, $\beta = 10$, $l/L = 10$, $\alpha = 0$. (*a*) $\tau = 1$, (*b*) 2, (*c*) 3.

5. Sample results for two ships

As was pointed out in §3, under the stated assumptions the total blockage of the ship is the primary parameter. Thus two similar ships moving side by side have the same effect as one ship with the length of the larger ship and the width of both. It is therefore more interesting to examine two ships in tandem. A comprehensive study would be very lengthy since the additional parameters are numerous (length ratio, width ratio, ship-to-ship spacing or speed difference). In figures 7–9 we present some results only for two identical ships spaced at 5 ship lengths ($10L$) from mid-ship to mid-ship. The half-beam of each ship is a parabola, the dimensionless length of the ships is 2 and the mid-ship sections are at $x = \pm 5$. Only three speeds are included.

At a subcritical speed, at small time large waves are independently generated ahead of the two bows. As time progresses solitons are formed ahead of the leading ship; between the ships large-amplitude oscillations are trapped. As the speed increases past the critical value, upstream solitons become higher. At sufficiently high supercritical speed no solitons are generated.

6. Conclusion

We have shown in this paper that a slender ship advancing near the critical speed in a shallow channel of finite width can radiate upstream solitons with crests

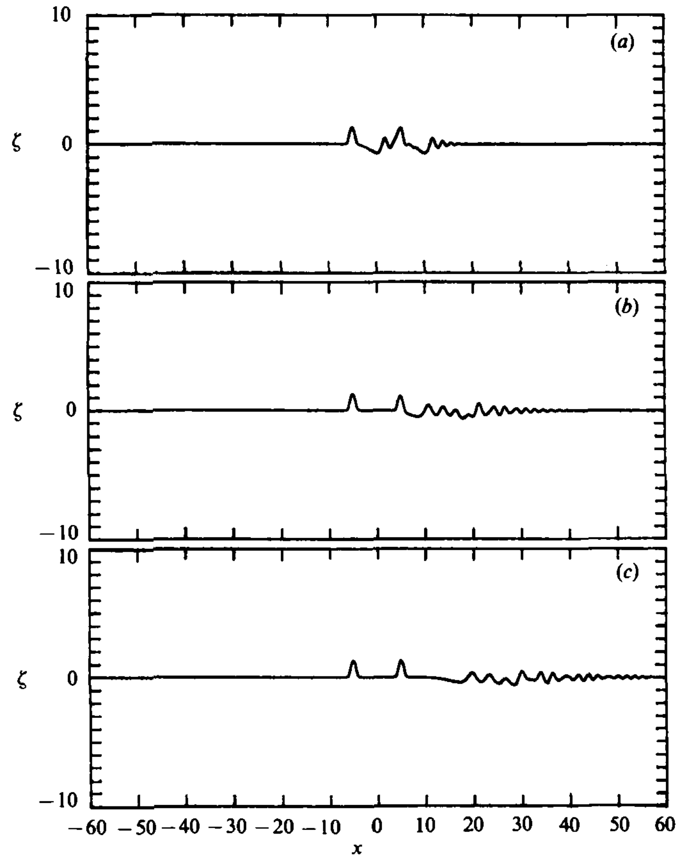

FIGURE 9. Evolution of free surface due to two identical ships in tandem, $\beta = 10$, $l = 10$, $\alpha = -2$. (a) $\tau = 1$, (b) 2, (c) 3.

transverse to the axis of the ship, and that these solitons are governed to leading order by a *one-dimensional* inhomogeneous KdV equation. Further study of a ship with small draught and beam is of interest to the theory of ship motion, and can be carried out by matched asymptotics; this will be reported elsewhere.

In other fluid systems where critical speeds exist, such as two-layered or continuously stratified fluids, upstream radiation of solitons may also arise when tides pass through a canal of varying cross-section, and this is worth investigation.

This research has been sponsored by the Fluid Mechanics programs of US Office of Naval Research (N00014-80-C-0531) and of US National Science Foundation (MEA7717817A04). Computer programs were kindly prepared by Mr. Ko-fei Liu. Comments by Professor J. V. Wehausen and Dr R. C. Ertekin of an earlier draft have been very helpful.

REFERENCES

AKYLAS, T. R. 1984 On the excitation of long nonlinear water waves by a moving pressure distribution. *J. Fluid Mech.* **141**, 455–466.

ERTEKIN, R. C. 1984 Soliton generation by moving disturbances in shallow water: theory, computation and experiment. Ph.D. thesis, Department Naval Arch., Offshore Engng, University of California, Berkeley.

Ertekin, R. C., Webster, W. C. & Wehausen, J. V. 1984 Ship-generated solitons. In *Proc. 15th Symp. Naval Hydrodyn., Hamburg.*

Graff, W. 1962 Untersuchungen über die Ausbildung des Wellenwiderstandes im Bereich der Stauwellengeschwindigkeit in flachem, seitlich beschränktem Fahrwasser. *Schifftechnik* **9**, 110–122.

Huang, D. B., Sibul, O. J., Webster, W. C., Wehausen, J. V., Wu, D. M. & Wu, T. Y. 1982 Ships moving in the transcritical range. In *Proc. Conference on Behavior of Ships in Restricted Waters, Varna, Bulgaria*, 26-1–26-9.

Johnson, R. S. 1972 Some numerical solutions of a variable coefficient Korteweg–de Vries equation. *J. Fluid Mech.* **54**, 81–91.

Kostyukov, A. A. 1968 *Theory of Ship Waves and Wave Resistance.* Iowa City, E.C.I.

Mei, C. C. 1976 Flow around a thin body moving in shallow water. *J. Fluid Mech.* **77**, 737–751.

Schmidt-Stiebitz, H. 1966 Die Abhängigkeit des Schiffswiderstandes von flachwasserbedingten Umströmungs- und Wasserspiegelveränderungen. *Schiff und Hafen* **18** (6), 381–395.

Thews, J. G. & Landweber, L. 1935 The influence of shallow water on the resistance of a cruiser model. *US Experimental Model Basin, Navy Yard, Washington, D.C. Rep. No.* 408.

Thews, J. G. & Landweber, L. 1936 A thirty-inch model of the S.S. Clairton in shallow water. *US Experimental Model Basin, Navy Yard, Washington, D.C., Rep. No.* 414.

Wehausen, J. V. & Laitone, E. V. 1960 Surface waves. *Handbuch der Physik*, vol. 9. Springer.

Wu, D. M. & Wu, T. Y. 1982 Three-dimensional nonlinear long waves due to moving surface pressure. In *Proc. 14th Symp. Naval Hydrodyn.*, 103–129.